Earthquake forecasting model for Albania: the area source model and the smoothing model

Edlira Xhafaj[1,2,3], Chung-Han Chan[3,4], Kuo-Fong Ma[1,2,3]

[1]Taiwan International Graduate Program (TIGP)–Earth System Science Program, Academia Sinica and National Central University, Academia Sinica, Taipei 11529, Taiwan
[2]Institute of Earth Sciences, Academia Sinica, Taipei 11529, Taiwan
[3]Earthquake-Disaster & Risk Evaluation and Management (E-DREaM) Center, National Central University, Taoyuan, 32001, Taiwan
[4]Department of Earth Sciences, National Central University, Taoyuan, 32001, Taiwan

Correspondence to: Chung-Han Chan (hantijun@googlemail.com)

Abstract. We proposed earthquake forecasting models for Albania, one of the most seismogenic regions in Europe, to give an overview of seismic activity by implementing area source and smoothing approaches. The earthquake catalog was first declustered to remove foreshocks and aftershocks when they are within the derived distance- and time-windows of mainshocks. Considering catalog completeness, the events with M≥4.1 during the period of 1960–2006 were implemented for the forecast model learning. The forecasting is implemented into an area source model that includes 20 sub-regions and a smoothing model with a cell size of 0.2˚ x 0.2˚ to forecast the seismicity in Albania. Both models show high seismic rates along the western coastline and in the southern part of the study area, consistent with previous studies that discussed seismicity in the area and currently active regions. To further validate the forecast performance of the two models, we introduced the Molchan diagram to quantify the correlation between models and observations. The Molchan diagram suggests that both models are significantly better than a random distribution, confirming their forecasting abilities. Our results provide crucial information for subsequent research on seismic activity, such as probabilistic seismic hazard assessment.

1. Introduction

Albania, located in the Balkan Peninsula, belongs to the Alpine-Mediterranean seismic belt, one of the most seismic regions in Europe, often threatened by devastating earthquakes, along with Turkey

and Greece (Aliaj et al., 2004; Sulstarova, 1996). High seismicity activity in the region has been the main scope of many researchers from Albanian and other experts, which includes Albania as part of their seismic hazard analysis (e.g., Aliaj et al., 2010, 2004; Fundo et al., 2012; Muco et al., 2012; Shebalin et al., 1974; Slejko et al., 1999; Sulstarova, 1996), as well as multinational programs and projects within Europe, the Balkans, and the Mediterranean region (e.g., Giardini, 1999; Jimenez et al., 2003; Jiménez et al., 2001; Salic et al., 2018; Woessner et al., 2015). So far, however, no controlled research has been conducted in Albania to investigate the correlation between seismic models.

There are two primary aims of this study: (1) to investigate earthquake forecasting in Albania using different models, and (2) to assure the credibility of these models. We focus on the seismic activity considering shallow crust events, which in the Albanian case, are generally at a depth of 10–20 km and, in many cases, near the surface (Sulstarova, 1996). The Albanian Seismological Network (ASN) data regarding the events from 1976 to 2000 shows that 95% of earthquakes had depths of less than 30 km (Muco, 2002). We investigate the seismicity of events that occurred in the region from 1960 to 2006 using the 2013 European Seismic Hazard Model (ESHM13) in the framework of the Seismic Hazard Harmonization in Europe project (referred to as SHARE), based on the SHARE European Earthquake Catalogue (SHEEC). By analyzing the catalog, we aim to propose earthquake forecasting models that can be used for future research to understand the seismicity in the area and compare them with models that include an extended catalog and seismogenic sources that are not incorporated into our forecasting model.

The time period of 46 years was chosen after the catalog is declustered according to the Gardner and Knopoff (1974) window method to evaluate the completeness time, threshold magnitude, and Gutenberg-Richter parameters (Gutenberg and Richter, 1944) Based on the catalog, we can forecast Albanian seismicity by implementing two models: the standard (Cornell, 1968) approach based on the area source model and the smoothing model by (Frankel, 1995). Area source polygons are defined by the ESHM13, designed with the assumption that seismicity may occur anywhere within each zone, and the delineation considers seismicity, tectonics, geology, and geodesy (Woessner et al., 2015). To avoid subjective judgments regarding how area source polygons are designed, a smoothing model is an

55 alternative approach used to forecast seismicity. The method is based on the principle that the distribution of past events can be used to predict where future events may occur (Frankel, 1995).

Both models demonstrate a high seismic rate along the western coastline and southern part of the study area, consistent with previous studies (Aliaj et al., 2004; Aliaj et al., 2010; Fundo et al., 2012) and currently active regions. To further evaluate the forecasting results from the two models, we introduced

60 the Molchan diagram to investigate the correlation between models and observations. The catalog from 1960 to 2006 is regarded as the "learning period" for model construction, and the seismicity during 2015–2020 is the "testing period" for comparing and validating the results. In addition, the null hypothesis is applied to confirm the forecasting ability of the models, and the results are performed for events according to each of the threshold magnitudes, which confirms the good forecasting ability of

65 both models. Finally, the results obtained from comparing the learning and testing periods are presented and discussed.

2. Earthquake catalog and analyzes

2.1 Catalog dataset

To analyze the seismicity, our area of study is bounded between the latitude of 38.0ºN-44.5ºN

70 and the longitude of 18.0ºE-23.0ºE (Fig. 1), and a seismicity working file is created for further analysis. The SHEEC catalog between 1900 and 2006 was compiled by the German Research Center for Geosciences (GFZ, Potsdam) and released as part of an independent project, representing a spatial-temporal extract from the "European-Mediterranean Earthquake Catalogue (EMEC, Grünthal et al., 2013; Grünthal & Wahlström, 2012)", which contains seismic events with moment magnitude from 3.5

75 to 7.0 for our region of study. We implemented events with a depth ≤ 35 km, considered shallow crustal events, according to previous studies (Muço, 1998; Slejko et al., 1999; Muco et al., 2002; Aliaj et al., 2004), and the ESHM13 (Woessner et al., 2015).

Figure 1: a) Map of epicenters of all the shallow earthquakes (depth ≤ 35 km) with magnitude Mw ≥ 3.5 for the period of time 1900-1959 represented by blue circles and the period 1960-2006 represented by purple circles. b) Annual seismic rate for the non declustered catalog with all the events occurred during the period 1900-1959, and annual seismic rate for the non-declustered catalog with all the events occurred during the period 1960-2006. Size of the circles corresponds to the magnitude of the earthquake, color codec accordingly the depth.

80   The catalog from 1900–2006 is considered to obtain completeness intervals for the entire study region using the cumulative number of events over time (Fig. 1a). When the slope changes, we consider the catalog complete for the magnitudes above reference (Duni et al., 2010; Markušić et al., 2016) , which are also consistent with the intervals obtained from applying the Stepp (1972) approach. The completeness intervals for the selected area are identified with a magnitude threshold of 4.1 for the

85   period 1974–2006 and completed events with a magnitude of 4.5 and 5.0 after 1950 and 1901, respectively. Duni et al. (2010) and Makropoulos et al. (2012) have reported similar completeness

intervals. Further analysis of this study focused on the period of time between 1960 to 2006 (Fig.2), a period during which the catalog is more complete and mainly based on instrumental data during the 20th century (Çağnan and Kalafat, 2012; Markušić et al., 2016).

90

2.2 Catalog declustering

Declustering earthquake catalog is a standard procedure for seismicity modeling, to keep only the mainshocks (the largest events in an earthquake sequence) and remove events identified as; foreshocks and aftershocks in a space-time window. The method is commonly used in engineering 95 seismology and statistical seismology, e.g., probabilistic seismic hazard assessment and earthquake forecasting. A variety of techniques for declustering a catalog to obtain background seismicity have been proposed; the majority of these methods eliminate earthquakes in a space-time window following a large occurrence known as the mainshock (Zhuang et al., 2002). The Gardner and Knopoff method (Gardner and Knopoff, 1974), also known as GK-1974, describes space-time windows dependent on the 100 magnitude of the mainshock and denotes events inside the window of a large event such as a foreshock or aftershock. The space and time window of the GK-1974 produces a declustered catalog that follows a Poisson distribution, which is not seen in other declustering methods (van Stiphout et al., 2012), and is presented as:

$$L\,(km) = 10^{0.1238\,\cdot\,M + 0.983}\,, \qquad T\,(days) = \begin{matrix} 10^{0.5409\,\cdot\,M\,-\,0.547}\,, if\,M < 6.5 \\ 10^{0.032\,\cdot\,M + 2.7389}\,, if\,M \geq 6.5 \end{matrix}\,, \text{respectively,}$$

105 (1)

where M is the magnitude of the mainshock, L is the distance from the mainshock in kilometers and T is the time in days. Given the moment magnitude of each earthquake in our catalog, using the algorithms from GK-1974, we calculated a specific distance L (M) and time T (M) to denote the foreshock and aftershock that took place before and after the mainshock, respectively. All the events are 110 sorted according to their magnitudes (highest to lowest), and those events that are within the spatial and temporal window of large events are dependent. Our forecasting models are conducted using only

mainshocks, as considering dependent events (foreshocks and aftershocks) would lead to a higher seismicity rate (e.g., Chan, 2016).
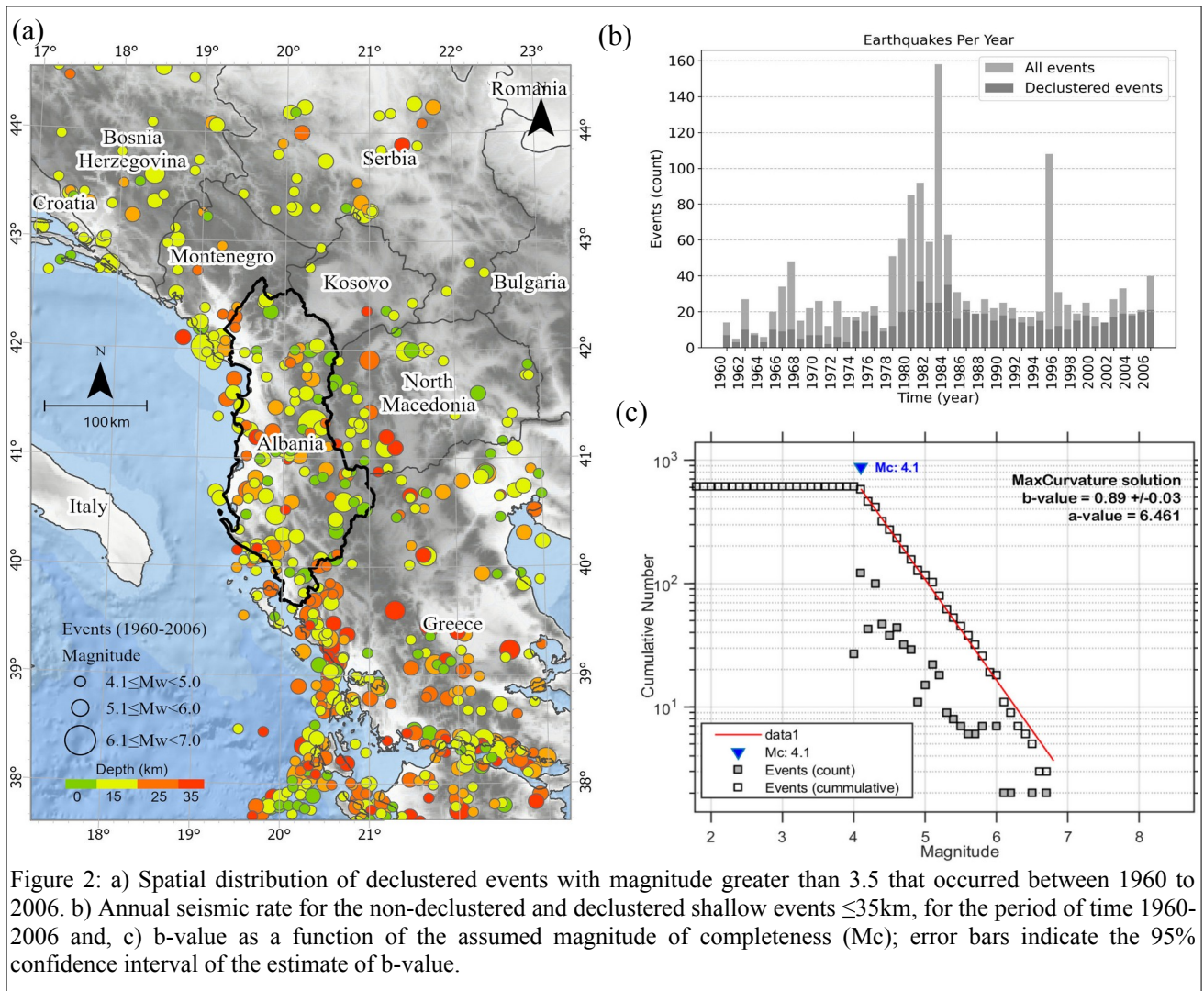
Figure 2: a) Spatial distribution of declustered events with magnitude greater than 3.5 that occurred between 1960 to 2006. b) Annual seismic rate for the non-declustered and declustered shallow events ≤35km, for the period of time 1960-2006 and, c) b-value as a function of the assumed magnitude of completeness (Mc); error bars indicate the 95% confidence interval of the estimate of b-value.

115 2.3 The magnitude of completeness (Mc)

The magnitude of completeness is defined as the minimum magnitude above which all earthquakes are reliably recorded and the value varies over time and space. Mc could be estimated based on the Gutenberg-Richter Law (Gutenberg and Richter, 1944), classifying earthquakes into the

number of occurrences with magnitudes greater than a given reference magnitude. The magnitude-frequency relation, the Gutenberg-Richter Law, is performed as follows:

$$logN(M) = a - b * M \text{ ,} \tag{2}$$

where N(M) is the number of earthquakes per year for a magnitude equal to M or larger than M, a-value (activity rate) represents the total seismic activity for a given seismic source (logN(M) for M≥0), and b-value represents the ratio between small and large events.

Identification of the completeness magnitude of an earthquake catalog is a clear requirement for the processing of input data for seismic hazard analysis. The complete part of the declustered SHEEC is an input to estimate the spatial and magnitude probability density of seismicity in the region, the same as the approach used to obtain the seismicity density for the entire Europe (Hiemer et al., 2014).

The declustered catalog for our area of study is divided into 0.1 magnitude bin intervals with a minimal magnitude of 4.0 and time bins of 1.0 years starting in 1960. For our study area, the magnitude of completeness Mc=4.1 from the Gutenberg-Richter relation was obtained based on the maximum curvature method and the goodness-of-fit test on the ZMAP software (Wiemer, 2001), and with an estimate of a=5.83 and b=0.87 value for the entire region of study (Fig.2c). The b-value obtained in this study is consistent with those by Grünthal et al. (2010), who reported the b-value range of 0.87 to 0.91 for a superzone covering Albania.

3. Earthquake forecasting models

An earthquake source model is an established approach to forecasting earthquake occurrences based on seismological, geological, tectonic, and geodetic data, with varying degrees of importance represented in the source typologies. The basic component of the forecasting model is an earthquake source model that determines the rate of earthquake activity and the rate of occurrence of events as a function of space, time, and magnitude (Hiemer et al., 2014). Here, we propose two forecasting models: the area source and smoothing models, detailed below.

3.1 The area source model

Area source models are one of the most implemented approaches to assessing seismic hazards
145 and characterizing seismicity that occurs over large regions where single fault structure detection and
classification, determination of location, geometry, and seismicity frequency parameters are difficult
(Wiemer et al., 2009). Our study area is covered by 20 area source polygons as proposed by ESHM13
(Fig. 3a), and those areas with few events have been merged into areas with similar characteristics.
Seismicity activity in the form of a- and b-values (Gutenberg and Richter, 1944), the annual rate of
150 seismic activity, and the maximum magnitude (Mmax) are evaluated for each of the area sources as
given in Table 1.

Table 1: Area sources parameters for our region of study, seismicity rate given in the Fig.3. *Area IDAS are the same as
those given by ESHM13 for each of the areas (the IDAS of the area with more events in kept over other merged area).

ID	IDAS	TECTONICS	No. Events	Area (km2)	a	b	Mmax (Inferred)
1	ALAS179	Active Shallow Crust	41	15062.45	4.99 (±0.075)	0.87 (± 0.03)	6.3
2	MKAS180	Active Shallow Crust	30	7682.46	4.82 (±0.097)		6.9
3	YUAS184	Active Shallow Crust	22	17080.75	4.52 (±0.125)		5.9
4	MKAS187	Active Shallow Crust	23	15883.98	4.47 (±0.139)		6.2
5	BAAS191	Active Shallow Crust	54	22471.91	4.96 (±0.076)		5.7
6	BAAS192	Active Shallow Crust	70	72463.77	5.04 (±0.073)		6
7	ITAS312	Active Shallow Crust	10	128205.13	4.16 (±0.176)		4.8
8	GRAS369	Active Shallow Crust	108	27108.43	5.50 (±0.045)		6.6
9	GRAS370	Active Shallow Crust	20	4437.54	4.71 (±0.103)		6.2
10	GRAS375	Active Shallow Crust	20	10204.08	4.77 (±0.082)		5.9
11	GRAS384	Active Shallow Crust	21	5844.7	5.37 (±0.052)		6.7
12	GRAS385	Active Shallow Crust	10	17123.29	4.47 (±0.125)		6.2
13	GRAS386	Active Shallow Crust	21	8267.72	4.79 (±0.079)		6.2
14	GRAS387	Active Shallow Crust	21	22604.95	4.82 (±0.090)		6.7
15	GRAS388	Active Shallow Crust	19	17304.19	4.74 (±0.090)		6.3
16	HRAS995	Active Shallow Crust	41	17998.24	4.92 (±0.078)		6.9
17	ALAS993	Active Shallow Crust	37	19151.14	4.82 (±0.090)		5.9

18	ALAS992	Active Shallow Crust	59	24614.1	5.17 (±0.062)		6.7
19	YUAS990	Active Shallow Crust	15	42372.88	4.91 (±0.055)		6.4
20	GRAS371	Active Shallow Crust	68	17694.51	5.06 (±0.055)		7

Since there is an insufficient number of events in some areas to obtain reliable Gutenberg-Richter parameters, we considered a fixed b = 0.87 for the entire region (Fig. 2c), which is used to define the a-value for each of the areas. A uniform b-value for all the area sources is sometimes implemented by probabilistic seismic hazard assessment to minimize the effect of zonation and a low number of events inside each individual area (e.g., Chan et al., 2020; Fujiwara et al., 2013). The a-value, which represents the overall activity of the seismic source, is calculated based on the unified b-value (Table 1). The annual rate for each area source is estimated to forecast the number of events with different magnitudes within each of them and the seismicity rate per km2 is plotted as given in Fig. 3a.

The maximum magnitude (Mmax) for each area was estimated from the maximum observed magnitude in the catalog using the method proposed by Kijko & Sellevoll (1992) and Fundo et al. (2012). As shown in Table 1, the area source GRAS371 (ID20) has the largest maximum magnitude in the catalog, with a Mmax of 7.0. Duni et al., (2010) for the area including the territory of Albania, concluded that the maximum magnitude was Mmax = 7.2 and Mmax = 6.9 for the historical and instrumental periods, respectively.
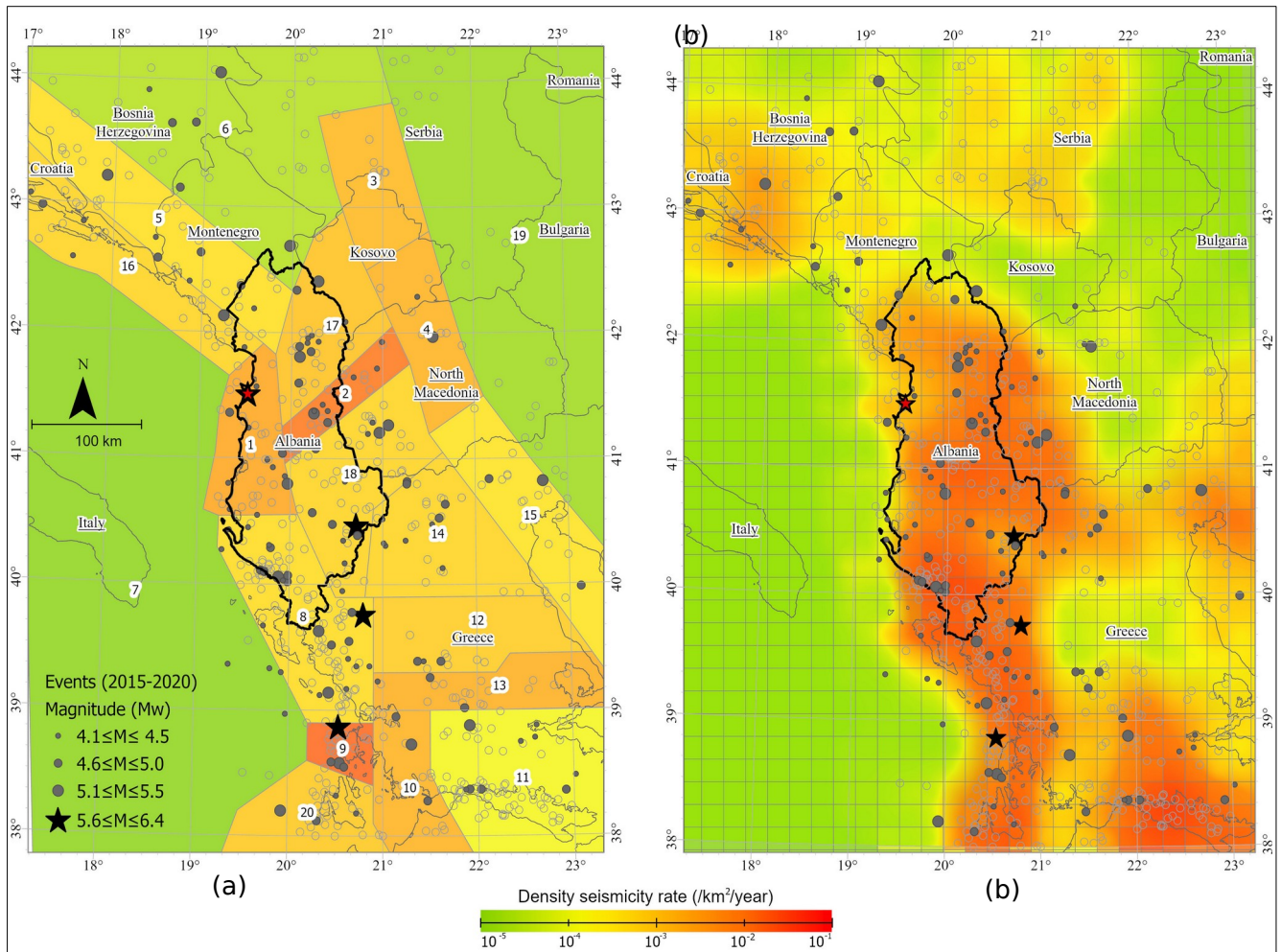
Figure 3: Density seismicity rate for the period 1960-2006 evaluated : a) area source model and b) smoothing model. Stars and grey filled circles with various sizes represent the events different magnitudes occurred during the "testing period" in 2015-2020 (from the IGS catalog). Grey open circles in background denotes the events occurred during the "learning period" from SHEEC (1960-2006). Numbers represent the ID labels for each area source as Table 1, red star denotes the 2019 Mw6.4 event.

3.2 The smoothing model

Besides the area source model, another seismogenic source model based on the smoothing
170 kernel, as proposed by Frankel (1995), is used for earthquake forecasting. The same approach is used to obtain the smoothed seismicity rates for the Harmonization of Seismic Hazard Maps in the Western Balkan Countries Project – BSHAP, (Salic et al., 2018). The method applies a simple isotropic Gaussian

smoothing kernel to derive the expected rate of events at each cell from the observed rate of seismicity in a grid of cells with a correlation distance c, represented as:

175

$$\tilde{n}_i = \frac{\sum n_j e^{d_{ij}^2/c^2}}{\sum e^{d_{ij}^2/c^2}}$$

(3)

where $\tilde{n}_i$ is the expected rate of events at each cell, n_j is the observed rate of seismicity in a grid of j cells, d^{ij} is the distance between the ith and j^{th} cells, and c is the correlation distance for the adaptive kernel, that indicates the bandwidth parameter of the Gaussian function that controls how rapidly the kernel's weights (seismicity) diminish with distance from its centre (number of events concentrated within a 0.2˚x 0.2˚ grid cell). Input parameters are the grid extend and grid cell size, the uniform b-value, bandwidth (in kilometers), completeness magnitude, and completeness year. The computed result is the observed number of earthquakes in each cell and the smoothed seismicity rate.

To apply the method, the area of study is divided into grid cells with a size of 0.2˚x 0.2˚, and the rate of earthquakes ($\tilde{n}_i$) with M≥4.1 is counted for each cell, this count represents the maximum likelihood estimate for that cell based on the method by Weichert (1980). The grid size 0.2˚x 0.2˚ is based on the events' location uncertainty as given by ESHM13 at the range of 10 to 15 km (Woessner et al., 2011). To apply the smoothing model, we follow the procedure (code) in Hazard Modeller's Toolkit, an open-source library that is related to the OpenQuake-engine hazard calculation software (Weatherill et al., 2014).

In this study, the correlation distance is fixed at 50km after testing different bandwidth values of 25 km and 50 km. As indicated in the original work by Frankel (1995), a larger than 50 km correlation distance spread out the seismicity so that details were lost, and smaller correlation distances resulted in segmented patterns of seismicity. The annual rates from the smoothed model were obtained for both bandwidths, and we show the compared forecasted seismicity rates in Fig. 4. The annual rates from the smoothed model for the bandwidth of 50 km (shown in Fig. 3b) forecast the highest seismicity rate in the south and west of the study area, where the largest number of events is located and moderate-to-large earthquakes have occurred.
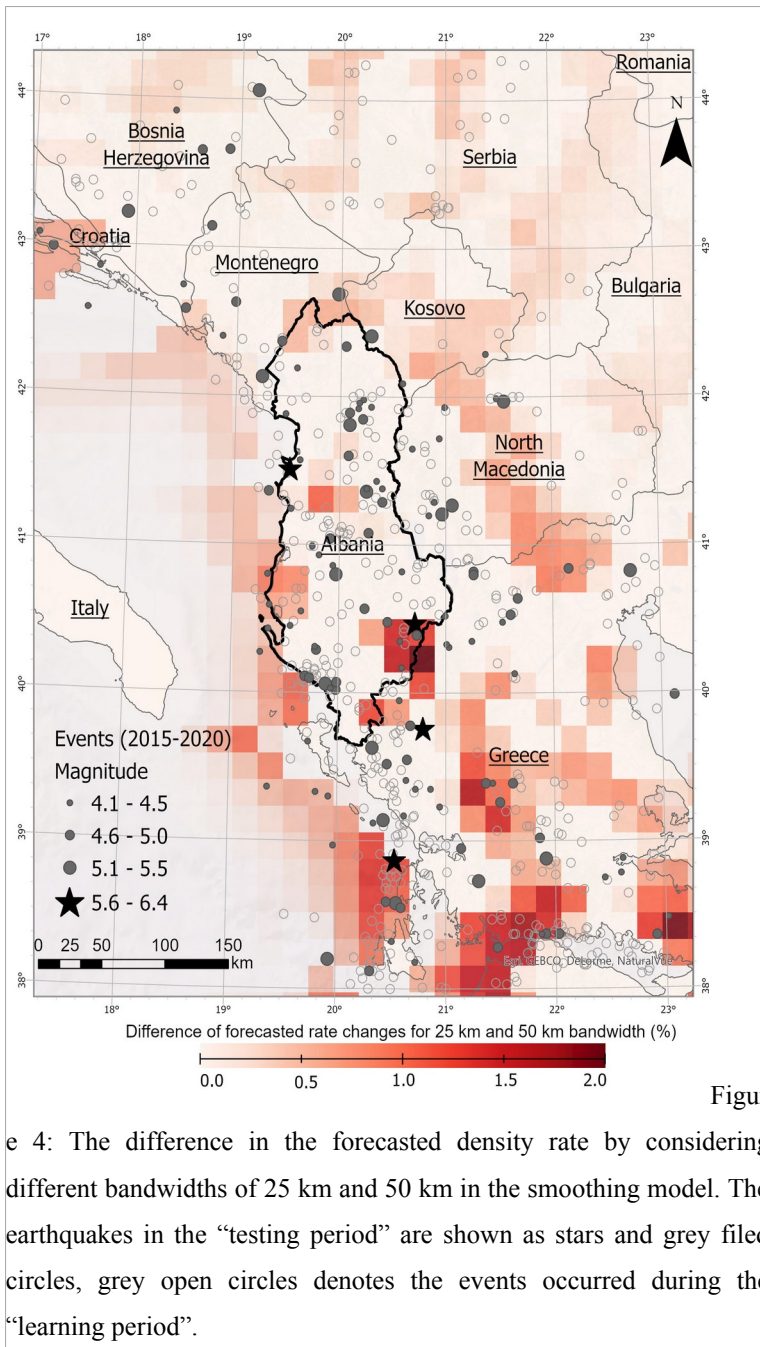
3.3 Model validation

To validate the performance of the models, the Molchan diagram approach is used (Molchan, 1990; Zechar and Jordan, 2008). This method aims to quantify forecasting ability by investigating the correlation or relationship between a model and observations of earthquake events. After obtaining the seismicity for the study region from the area source and the smoothing model, we proceed to forecast the spatial distribution of seismic events spanning the period from 2015 to 2020. The dataset integrates catalog and the bulletins provided by the Institute of Geo-Science of Albania, referred to as the 'IGS catalog.' Specifically, events with magnitudes equal to or greater than 4.1 are depicted as grey dots, while events with a magnitude of 5.0 or higher are represented by

Figure 4: The difference in the forecasted density rate by considering different bandwidths of 25 km and 50 km in the smoothing model. The earthquakes in the "testing period" are shown as stars and grey filed circles, grey open circles denotes the events occurred during the "learning period".

black stars, as illustrated in Figure 3. The reported event's magnitude from IGS is local magnitude (M_L), and the conversion to moment magnitude (Mw) follows the relevant regression equations by Duni et al., (2010):

$$M_w = 1.624 + 0.743M_L \qquad\qquad (4)$$

One of the largest events in this period in the territory of Albania was recorded along the coastline, which occurred on November 26, 2019, with Mw6.4, the most destructive earthquake in the western part of the country. The area of study is divided into grid cells $0.2° \times 0.2°$ to obtain and validate the seismicity for each of the catalogs through the area source model and smoothing model. We have defined the catalog from SHEEC (1960–2006) as the "learning" catalog and the IGS (2015-2020) as the "testing" catalog. Both catalogs were declustered with the same window method by Gardner and Knopoff (1974) for shallow crustal events, as we prefer to follow similar analysis procedures for a better evaluation of our data and models. For the "testing" catalog, we have determined the fraction of alarm-occupied space as the percentage of observations within the region with a forecasting level equal to or higher than "alarm", and the fraction of failure in forecasting as the percentage of observations having a lower forecasting level than "alarm". Since the study region is divided into grid cells, each cell in which an earthquake is forecast to occur constitutes an alarm cell.

A Molchan diagram plots the missing rate versus the alarming rate and each of them gets a value from 0 to 1 (0% to 100%). If the alarming rate changes from 0 to 1, the missing rate will decrease from 1 to 0. The diagonal line from (0,1) to (1,0) would be the long-run expectation for alarms that are declared randomly, i.e., the missing rate equals the alarming rate, indicating a completely random guess. A perfect forecast would have a value of missing alarm equal to 0 (no false alarms) and an alarm equal to 1, that is all earthquakes are perfectly forecasted (Molchan, 1990, 1991). The prediction points under the diagonal line mean the missing rate is less than the alarming rate and the prediction is better than a random guess, which is consistent with our analysis as they follow the definition given for the evaluation of source models with the Molchan diagram. We underlined that both diagrams show good performance for the targeted observations but are more suitable for large events. Also, the smoothed model indicates a better forecast for future events than the area source model, as the predictive curve is always lower than the area source model's predictive curve.

The forecasting performance of different source models is investigated by plotting the curve at a 99% confidence interval of the null hypothesis for the forecasting events with M≥4.1 and M≥5.0 (shown in Fig. 5a and b, respectively), confirming the good forecasting performance of the area source

and smoothing model as both respective curves are under the confidence interval curve. As discussed by
255   Schorlemmer et al. (2010), assuming a null hypothesis where the observations fall into the lower curve
of the distribution, the null hypothesis is rejected.
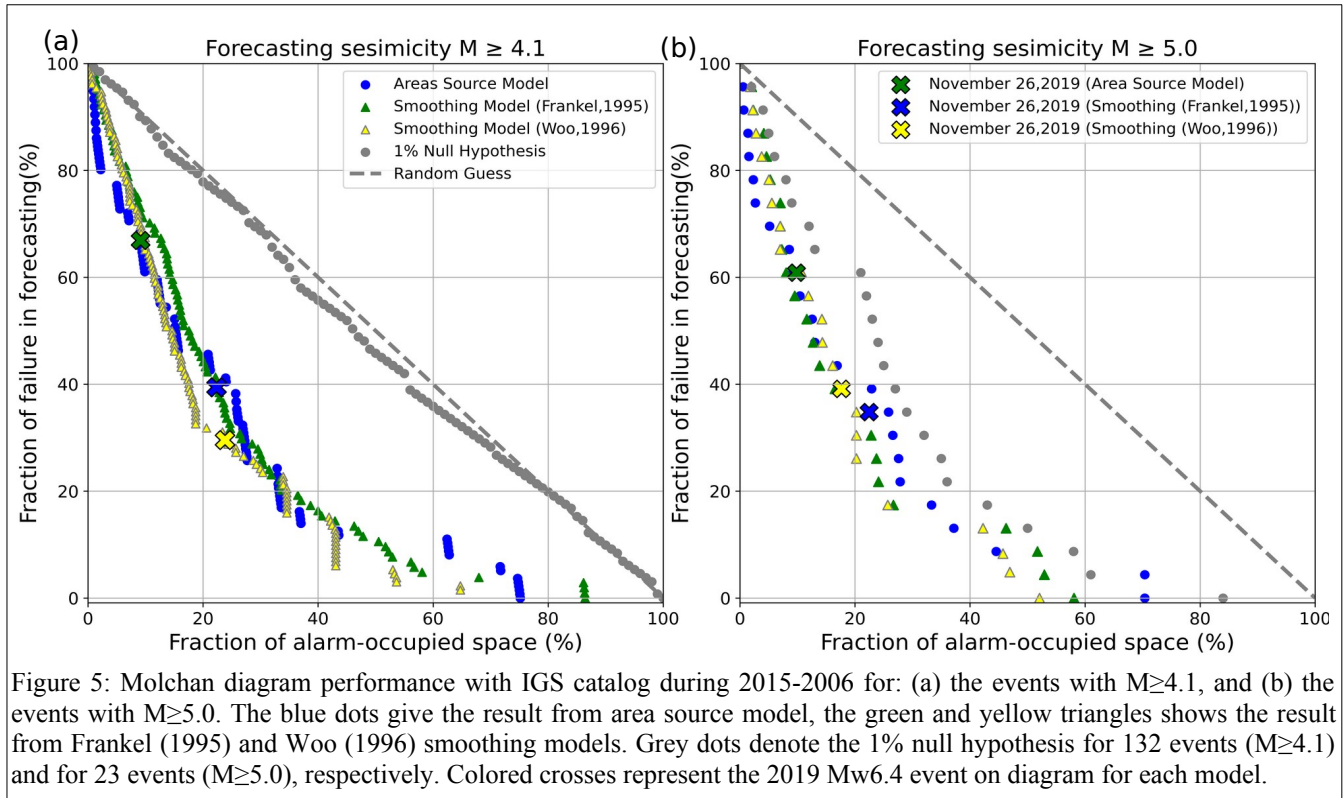
Figure 5: Molchan diagram performance with IGS catalog during 2015-2006 for: (a) the events with M≥4.1, and (b) the
events with M≥5.0. The blue dots give the result from area source model, the green and yellow triangles shows the result
from Frankel (1995) and Woo (1996) smoothing models. Grey dots denote the 1% null hypothesis for 132 events (M≥4.1)
and for 23 events (M≥5.0), respectively. Colored crosses represent the 2019 Mw6.4 event on diagram for each model.

4. Discussion and conclusions

260   The present study was designed to propose earthquake forecasting models and to discuss the
seismic activity in one of the most seismic regions on the European continent, using past earthquakes to
forecast future earthquakes. Two distinct forecasting methodologies were employed to establish the
geographical pattern of seismic activity, focusing on events with a minimum magnitude of 4.1, which
marks the completeness threshold of the earthquake catalog. The boundary is lower than the minimum
265   magnitude (Mmin = 4.5) considered by Fundo et al. (2012), as the low bound for building damage. The
annual seismicity rate for our forecasting models is determined from the complete part of the
declustered earthquake catalog, taking into account a- and b-values and the distribution of maximum

magnitude (Mmax). The highest seismic activity rate is forecasted along the western coastline and southern part of the study region, which corresponds to the location of observed earthquakes as given by

270 the earthquake catalog, compared to the low activity rates in the central part (area source 17 and 18 for Albania, other low-density areas, refer Fig.3a) of the study region. The seismic rate calculated from both models, depicted in Figure 3, aligns with earlier research on seismic activity, as documented by Slejko et al. (1999), Aliaj et al. (2004), Fundo et al. (2012), Salic et al. (2018), and Woessner et al. (2015).

275 To evaluate the smoothing model's uncertainty and the impact of bandwidths, we compared the forecasted seismicity rates corresponding to two different bandwidths of 25 km and 50 km, which are comparable to the events' location uncertainty described in Section 3.2. The contrast in rates between the smoothing seismicity from difference bandwidths reveals that variations are trivial, with an overall deviation of less than 2% across the entire study area. Furthermore, both models exhibit a high level of

280 confidence, exceeding 98% probability, as depicted in Figure 4. Note that most of the forecast events are in the region, with an insignificant difference in the seismicity rate. When we compare our models with observations as given by IGS, the higher seismicity rate is highlighted along the coastline (Fig. 3). The maximum magnitude based on the observed events has a value of 6.8, which is comparable to Mmax = 6.9, claimed by Duni et al., (2010) as the maximum magnitude for the instrumental period in

285 Albania for the catalog period from 510 BC to 2008 AD, proving that our estimations for Mmax obtained following the method proposed by Kijko & Sellevoll (1992) seem to be reasonable.

Furthermore, to test the consistency of the results from the area source and smoothing model, the credibility of our models was confirmed by the Molchan diagram, as all the events from the testing catalog (represented by grey dots and black stars in Figs. 3 and 4) are under the diagonal line, approving

290 the good forecasting abilities of both approaches. The models show better forecasting ability for larger events with M≥5.0 than smaller ones with M≥4.1 (Fig. 5). Many of the events occur in areas where both earthquake source models have high forecasting rates, and such a conclusion is crucial for probabilistic seismic hazard assessment. We present the location of the November 26, 2019 (Mw6.4) event (black stars, in Figs. 3 and 4) that occurred in the western part of Albania on the Molchan diagram, which

295 appears to have a low fraction of alarm-occupied space compared to the smoothing model, confirming

again a better forecasting performance compared to the forecasting performance from the area source model (Fig. 5).

The smoothing kernel approach of Frankel (1995) implemented in this study is magnitude-independent and the spatial distribution for large magnitudes could be forecasted based on the distribution of smaller events, providing better forecasting ability. We further propose another forecasting model using a magnitude-dependent smoothing approach proposed by Woo (1996). This approach has been applied to various studies (e.g., Chan et al., 2018). The findings are graphically presented for the purpose of comparison, along with the area source and Frenkel (1995) approach in Figure 5, revealing similar forecasting abilities between the three approaches. Findings regarding seismicity parameters and source models as presented above have significant implications for the understanding of seismic activity in our region and to raise awareness of earthquake phenomena.

Additional studies are desired for further investigation of the earthquake catalog, including a longer period, and to integrate supplementary data regarding other seismogenic sources from geological and tectonic information for the subsequent probabilistic seismic hazard assessment. This study can be used for future research work completed with information about fault activity, segmentation models, rupture process documentation, and seismic moment accumulation that are not incorporated into our forecasting model.

Data availability

The data (catalogs and area polygons) in this study are provided from the European Facilities for Earthquake Hazard and Risk (EFEHR) and are available online through the ESHM13 Overview on http://efehrcms.ethz.ch/en/Documentation/specific-hazard-models/europe/overview/. The SHEEC catalog (1900-2006) was compiled by the German Research Center for Geo-sciences (GFZ, Potsdam) and released under https://www.gfz-potsdam.de/emec/ as part of an independent project, representing a spatial-temporal extract from the "European-Mediterranean Earthquake Catalog (EMEC)". The 2013 Euro-Mediterranean Seismic Hazard Model (ESHM13) was developed within the SHARE Project, and more information can be found at http://www.share-eu.org/. The data for the period 2015-2020 are

collected combining the catalog and the bulletin data from the Institute of Geo-science of Albania (https://www.geo.edu.al/site/).

Acknowledgements

325   This study was supported by the Ministry of Science and Technology in Taiwan--under the grants MOST 109-2116-M-008-029-MY3, MOST 110-2124-M-002-008008, and MOST 110-2634-F-008-008. This work is financially supported by the Earthquake Disaster & Risk Evaluation and Management Center (E-DREaM) from the Featured Areas Research Center Program within the framework of the Higher Education Sprout Project by the Ministry of Education in Taiwan.

330

References

Aliaj, S., Adams, J., Halchuk, S., Sulstarova, E., Peçi, V., and Muço, B.: Probabilistic seismic hazard maps for Albania, https://doi.org/10.4095/226354, 2004.

Aliaj, S., Kociu, S., Muco, B., and Sulstarova, E.: Seismicity, seismotectonics and seismic hazard assessment in Albania, 2010.

Çağnan, Z. and Kalafat, D.: A New Catalogue of Eastern Mediterranean Earthquakes, 2150 BC – 2011, 10, 2012.

Chan, C., Ma, K., Lee, Y., and Wang, Y.: Rethinking Seismic Source Model of Probabilistic Hazard Assessment in Taiwan after the 2018 Hualien, Taiwan, Earthquake Sequence, Seismological Research Letters, 90, 88–96, https://doi.org/10.1785/0220180225, 2018.

Chan, C.-H.: Importance of three-dimensional grids and time-dependent factors for applications of earthquake forecasting models to subduction environments, Natural Hazards and Earth System Sciences, 16, 2177–2187, https://doi.org/10.5194/nhess-16-2177-2016, 2016.

Chan, C.-H., Ma, K.-F., Shyu, J. B., Lee, Y.-T., Wang, Y.-J., Gao, J.-C., Yen, Y.-T., and Rau, R.-J.: Probabilistic seismic hazard assessment for Taiwan: TEM PSHA2020, Earthquake Spectra, 36, 875529302095158, https://doi.org/10.1177/8755293020951587, 2020.

Cornell, C. A.: Engineering seismic risk analysis, Bulletin of the Seismological Society of America, 58, 1583–1606, https://doi.org/10.1785/BSSA0580051583, 1968.

Duni, L., Kuka, N., Kuka, S., and Fundo, A.: Towards a New Seismic Hazard Assessment of Albania, in: 14th European Conference on Earthquake Engineering 2010, 14th European Conference on Earthquake Engineering 2010, Red Hook, NY, 8, 2010.

Frankel, A.: Mapping Seismic Hazard in the Central and Eastern United States, Seismological Research Letters, 66, 8–21, https://doi.org/10.1785/gssrl.66.4.8, 1995.

Fujiwara, H., Morikawa, N., and Okumura, T.: Seismic Hazard Assessment for Japan: Reconsiderations After the 2011 Tohoku Earthquake, Journal of Disaster Research, 8, 848–860, https://doi.org/10.20965/jdr.2013.p0848, 2013.

Fundo, A., Ll, D., Kuka, S., Begu, E., and Kuka, N.: Probabilistic seismic hazard assessment of Albania, Acta Geodaetica et Geophysica Hungarica, 47, 465–479, https://doi.org/10.1556/ageod.47.2012.4.7, 2012.

Gardner, J. K. and Knopoff, L.: Is the sequence of earthquakes in Southern California, with aftershocks removed, Poissonian?, Bulletin of the Seismological Society of America, 64, 1363–1367, https://doi.org/10.1785/BSSA0640051363, 1974.

Giardini, D.: The Global Seismic Hazard Assessment Program (GSHAP)-1992/1999, Annali di Geofisica, 42, https://doi.org/10.4401/ag-3780, 1999.

Grünthal, G. and Wahlström, R.: The European-Mediterranean Earthquake Catalogue (EMEC) for the last millennium, J Seismol, 16, 535–570, https://doi.org/10.1007/s10950-012-9302-y, 2012.

Grünthal, G., Arvidsson, R., and Bosse, C.: Earthquake model for the European-Mediterranean Region for the purpose of GEM1, 1–35, https://doi.org/10.2312/GFZ.b103-10043, 2010.

Grünthal, G., Wahlström, R., and Stromeyer, D.: The SHARE European Earthquake Catalogue (SHEEC) for the time period 1900–2006 and its comparison to the European-Mediterranean Earthquake Catalogue (EMEC), J Seismol, 17, 1339–1344, https://doi.org/10.1007/s10950-013-9379-y, 2013.

Gutenberg, B. and Richter, C. F.: Frequency of earthquakes in California*, Bulletin of the Seismological Society of America, 34, 185–188, https://doi.org/10.1785/BSSA0340040185, 1944.

Hiemer, S., Woessner, J., Basili, R., Danciu, L., Giardini, D., and Wiemer, S.: A smoothed stochastic earthquake rate model considering seismicity and fault moment release for Europe, Geophysical Journal International, 198, 1159–1172, https://doi.org/10.1093/gji/ggu186, 2014.

Jimenez, J., Giardini, D., and Grunthal, G.: The ESC-SESAME Unified Hazard Model for the European-Mediterranean region, 5, 2003.

Jiménez, M., D.Giardini, Grünthal, G., Erdik, M., García-Fernández, M., J.Lapajne, Makropoulos, K., R.Musson, Papaioannou, C., Rebez, A., Riad, S., Sellami, S., A.Shapira, Slejko, D., Eck, T., and Sayed, A. E.: Unified Seismic Hazard Modeling Throughout The Mediterranean Region, Bollettino di Geofisica Teorica ed Applicata, 3–18, 2001.

Kijko, A. and Sellevoll, M.: Estimation of earthquake hazard parameters from incomplete data files. Part II. Incorporation of magnitude heterogeneity, Bulletin of the Seismological Society of America, 82, 120–134, 1992.

Makropoulos, K., Kaviris, G., and Kouskouna, V.: An updated and extended earthquake catalogue for Greece and adjacent areas since 1900, Natural hazards and earth system sciences, 12, 1425–1430, https://doi.org/10.5194/nhess-12-1425-2012, 2012.

Markušić, S., Gülerce, Z., Kuka, N., Duni, L., Ivančić, I., Radovanović, S., Glavatović, B., Milutinović, Z., Akkar, S., Kovačević, S., Mihaljević, J., and Šalić, R.: An updated and unified earthquake catalogue for the Western Balkan Region, Bull Earthquake Eng, 14, 321–343, https://doi.org/10.1007/s10518-015-9833-z, 2016.

Molchan, G. M.: Strategies in strong earthquake prediction, Physics of the Earth and Planetary Interiors, 61, 84–98, https://doi.org/10.1016/0031-9201(90)90097-H, 1990.

Molchan, G. M.: Structure of optimal strategies in earthquake prediction, Tectonophysics, 193, 267–276, https://doi.org/10.1016/0040-1951(91)90336-Q, 1991.

Muco, B.: Development of a Moment Magnitude Relation for Albania, Bulletin of The Seismological Society of America - BULL SEISMOL SOC AMER, 92, 1136–1140, https://doi.org/10.1785/0120010204, 2002.

Muco, B., Alexiev, G., Aliaj, S., Elezi, Z., Grecu, B., Mandrescu, N., Milutinovic, Z., Radulian, M., Ranguelov, B., and Shkupi, D.: Geohazards assessment and mapping of some Balkan countries, NATURAL HAZARDS, 64, 943–981, https://doi.org/10.1007/s11069-012-0185-6, 2012.

Salic, R., Gulerce, Z., Kuka, N., Markušić, S., Mihaljevic, J., Kovačević, V., Sandikkaya, M. A., Milutinovic, Z., Duni, L., Stanko, D., Kaludjerovic, N., and Kovačević, S.: Harmonized seismic hazard maps for the western Balkan countries, in: 16th European Conference on Earthquake Engineering, 16th European Conference on Earthquake Engineering, Thessaloniki, Greece, 2018.

Schorlemmer, D., Zechar, J. D., Werner, M. J., Field, E. H., Jackson, D. D., Jordan, T. H., and the RELM Working Group: First Results of the Regional Earthquake Likelihood Models Experiment, Pure Appl. Geophys., 167, 859–876, https://doi.org/10.1007/s00024-010-0081-5, 2010.

Shebalin, N. V., Karnik, V., and Hadzievski, D.: Catalogue of earthquakes of the Balkan region, 1974.

Slejko, D., Camassi, R., Cecic, I., Muço, B., and Herak, D.: Seismic hazard assessment for Adria, 1999.

van Stiphout, T., Zhuang, J., and Marsan, D.: Seismicity declustering, Community Online Resource for Statistical Seismicity Analysis, 25, https://doi.org/10.5078/corssa52382934, 2012.

Sulstarova, E.: Earthquake hazard assessment in Albania, in: Risque, nature et société : Actes du séminaire « Delphes I », edited by: Faugères, L. and Villain-Gandossi, C., Éditions de la Sorbonne, Paris, 199–216, 1996.

Weatherill, G., Rodríguez, L., and Pagani, M.: The seismic hazard modeller's toolkit: An open-source library for the construction of probabilistic seismic hazard models, 2014.

Weichert, D. H.: Estimation of the earthquake recurrence parameters for unequal observation periods for different magnitudes, Bulletin of the Seismological Society of America, 70, 1337–1346, https://doi.org/10.1785/BSSA0700041337, 1980.

Wiemer, S.: A Software Package to Analyze Seismicity: ZMAP, Seismological Research Letters, 72, 373–382, https://doi.org/10.1785/gssrl.72.3.373, 2001.

Wiemer, S., García-Fernández, M., and Burg, J.-P.: Development of a seismic source model for probabilistic seismic hazard assessment of nuclear power plant sites in Switzerland: the view from PEGASOS Expert Group 4 (EG1d), Swiss J. Geosci., 102, 189–209, https://doi.org/10.1007/s00015-009-1311-7, 2009.

Woessner, J., Laurentiu, D., Giardini, D., Crowley, H., Cotton, F., Grünthal, G., Valensise, G., Arvidsson, R., Basili, R., Demircioglu, M. B., Hiemer, S., Meletti, C., Musson, R. W., Rovida, A. N., Sesetyan, K., Stucchi, M., and The SHARE Consortium: The 2013 European Seismic Hazard Model: key components and results, Bull Earthquake Eng, 13, 3553–3596, https://doi.org/10.1007/s10518-015-9795-1, 2015.

Woo, G.: Kernel estimation methods for seismic hazard area source modeling, Bulletin of the Seismological Society of America, 86, 353–362, https://doi.org/10.1785/BSSA0860020353, 1996.

Zechar, J. D. and Jordan, T. H.: Testing alarm-based earthquake predictions, Geophysical Journal International, 172, 715–724, https://doi.org/10.1111/j.1365-246X.2007.03676.x, 2008.

Zhuang, J., Ogata, Y., and Vere-Jones, D.: Stochastic Declustering of Space-Time Earthquake Occurrences, Journal of the American Statistical Association, 97, 369–380, https://doi.org/10.1198/016214502760046925, 2002.